J|A|C|S ARTICLES

Published on Web 05/27/2010

Static and Dynamic Electrowetting of an Ionic Liquid in a Solid/Liquid/Liquid System

Mani Paneru, Craig Priest, Rossen Sedev,* and John Ralston

Ian Wark Research Institute, ARC Special Research Centre for Particle and Material Interfaces, University of South Australia, Mawson Lakes, SA 5095, Australia

Received December 17, 2009; E-mail: rossen.sedev@unisa.edu.au

Abstract: A droplet of an ionic liquid (1-butyl-3-methylimidazolium tetrafluoroborate, bmim.BF_4) is immersed in an immiscible liquid (*n*-hexadecane) and electrowetted on a flat Teflon AF1600-coated ITO electrode. The static contact angle decreases significantly when voltage is applied between the droplet and the electrode: from 145° down to 50° (with DC voltage) and 15° (with AC voltage). The electrowetting curves (contact angle versus voltage) are similar to the ones obtained in other solid/liquid/vapor and solid/liquid/liquid systems: symmetric with respect to zero voltage and correctly described by Young-Lippmann equation below saturation. The reversibility is excellent and contact angle hysteresis is minimal (~2°). The step size used in applying the DC voltage and the polarity of the voltage are unimportant. The saturation contact angle cannot be predicted with the simple zero-interfacial tension theory. Spreading (after applying a DC voltage) and retraction (after switching off the voltage) of the droplet is monitored. The base area of the droplet varies exponentially during wetting (exponential saturation) and dewetting (exponential decay). The characteristic time is 20 ms for spreading and 35 ms for retraction (such asymmetry is not observed with water−glycerol mixtures of a similar viscosity). The spreading kinetics (dynamic contact angle versus contact line speed) can be described by the hydrodynamic model (Voinov's equation) for small contact angles and by the molecular-kinetic model (Blake's equation) for large contact angles. The role of viscous and molecular dissipation follows the scheme outlined by Brochard-Wyart and de Gennes.

Introduction

Electrowetting is the process of modifying the contact angle by applying an external electric field.[1−3] In the most common experimental configuration, an electrically conducting droplet rests on a relatively hydrophobic insulated electrode. The insulating layer effectively fills a parallel plate capacitor (the electrode and the droplet being the plates of this capacitor) and can be charged when external potential is applied. Charge carriers from within the liquid will accumulate at the solid/liquid interface and reduce the effective solid/liquid interfacial tension. This in turn, decreases the macroscopic contact angle, which becomes a function of the applied voltage.

Electrowetting is well described by the Young-Lippmann equation[1−3] which expresses the contact angle, θ, as a function of the applied voltage, V:

$$\cos\theta = \cos\theta_0 + \frac{\varepsilon\varepsilon_0}{2\gamma d}V^2 \qquad (1)$$

The dielectric constant of the insulating material is ε, ε_0 is the permittivity of vacuum, γ is the interfacial tension of the liquid/fluid droplet interface, d is the thickness of the insulating layer, and θ_0 is the contact angle at zero potential. Equation 1 describes the electrowetting curve (contact angle versus voltage) very well, provided the applied potential does not exceed a specific threshold value, V_S, the saturation potential. At voltages larger than V_S, the contact angle does not follow the Young-Lippmann equation and becomes more or less independent of the applied voltage.

Contact angle saturation and contact angle hysteresis significantly limit the usefulness of electrowetting in practical situations. The physical mechanism of saturation is still a matter of debate. Mechanisms explaining contact angle saturation have been proposed: charge trapping at the solid surface,[4] ionization of the ambient fluid close to the contact line,[5] defects in the insulating layer,[6] nonzero liquid resistance,[7] and dielectric breakdown.[8,9] We have argued that the Young-Lippmann equation is valid up to $\gamma_{SL} = 0$ (where $V = V_S$), and this provides a prediction for the saturation angle:[2]

$$\cos\theta_S = \frac{\gamma_S}{\gamma} \qquad (2)$$

where γ_S is the surface tension of the solid. Equation 2 provides a reasonable estimate for fluoropolymer surfaces and several other cases (using the critical surface tension of wetting as an

(1) Welters, W. J. J.; Fokkink, L. G. J. *Langmuir* **1998**, *14*, 1535.
(2) Quinn, A.; Sedev, R.; Ralston, J. *J. Phys. Chem. B* **2005**, *109*, 6268.
(3) Mugele, F.; Baret, J.-C. *J. Phys.: Condens. Matter* **2005**, *17*, R705.
(4) Verheijen, H. J. J.; Prins, M. W. J. *Langmuir* **1999**, *15*, 6616.
(5) Vallet, M.; Vallade, M.; Berge, B. *Eur. Phys. J. B* **1999**, *11*, 583.
(6) Seyrat, E.; Hayes, R. A. *J. Appl. Phys.* **2001**, *90*, 1383.
(7) Shapiro, B.; Moon, H.; Garrell, R. L.; Kim, C.-J. *J. Appl. Phys.* **2003**, *93*, 5794.
(8) Papathanasiou, A. G.; Boudouvis, A. G. *Appl. Phys. Lett.* **2005**, *86*, 164102/1.
(9) Papathanasiou, A. G.; Papaioannou, A. T.; Boudouvis, A. G. *J. Appl. Phys.* **2008**, *103*, 034901/1.

approximation for γ_S). It estimates the point of deviation from the Young-Lippmann equation rather than the lowest achievable contact angle. More recently, electrowetting measurements in the presence of surfactants[10,11] have lent further support to the validity of the zero-interfacial-tension hypothesis.

Since electrowetting is a fast and easily implemented technique for electronic control of small amounts of liquid, a variety of devices have been developed, for example, optical switches,[12] microlenses,[13] microvalves,[14] triggers,[15] pixels[16−18] and micropumps.[19,20] A comprehensive review of what can be achieved through electrowetting in digital microfluidics has been presented by Fair.[21] In all these applications, frequent switching is involved, and therefore, the reversibility and robustness of the electrowetting effect are crucial.

Most of the work on electrowetting has been carried out with solid/liquid/air systems, usually a drop of electrolyte in ambient air.[3] Replacing air with an immiscible oil, however, offers a range of advantages[21] (no evaporation, lesser contamination, small contact angle hysteresis and therefore easier actuation and improved liquid transport) and solid/liquid/liquid systems have become rather popular. Janocha et al.[22] attempted electrowetting of a decane droplet immersed in water on several polymer surfaces with variable success. Berge and Peseux[13] used organic liquid droplets immersed in an aqueous solution of sodium sulfate. Quilliet and Berge[23] estimated theoretically that, under equilibrium conditions, a thin film of ambient oil (∼20 nm, stabilized by van der Waals forces) could be present under the water droplet. This oil film is essentially lubricating the water droplet and therefore responsible for the very low contact angle hysteresis seen in solid/liquid/liquid systems. This idea is found in microfluidic studies of a water droplet moving through an immiscible oil[24] or physiological fluids undergoing multiple-step manipulation on a single chip.[25] The ambient oil significantly reduces biofouling in microfluidics and is of key importance to this field.[21,25] Static and transient capacitance measurements have demonstrated convincingly the presence a wetting film of oil.[21] Berry and co-workers studied the electrowetting of aqueous droplets containing salt and surfactant in alkanes on an amorphous fluoropolymer surface.[10,11,26] Electrowetting experiments have been performed with mercury in salty water on mica.[27]

Staicu and Mugele[28] studied the dynamic entrapment of an oil film between an aqueous droplet and the insulating polymer layer. The film is unstable and breaks into droplets. The same effect provides opportunities to optimize the design of electrowetting display pixels.[18]

Ionic liquids are a new class of solvents made widely available only in recent years.[29−32] These are organic salts with relatively low melting points. Their fluidity, nonvolatility, and good thermal stability are attractive properties. Many diverse ionic liquids can be synthesized and their properties can be tailored. Ionic liquids are conductive and stable within a wide range of potentials.[33] We have shown previously that ionic liquids can electrowet fluoropolymer surfaces in air, though not very efficiently.[34] More recently, we have published details of the robust electrowetting behavior of bmim.BF_4−water mixtures on a fluoropolymer surface in ambient hexadecane.[35]

To implement the electrowetting effect for electronically controlled manipulation of ionic liquid droplets, it is crucial to examine the kinetics of spreading and retraction. When an external voltage is applied, the wettability of the solid substrate is instantly improved, and the droplet will spread until the contact angle reaches its final value. If the voltage is then switched off, the original wettability is restored, and the droplet will retract back to its initial shape. Under these conditions, the dynamic contact angle, θ, becomes a function of the speed of the contact line, u, with respect to the solid surface. The velocity dependence of the contact angle is usually described in terms of a hydrodynamic model or a molecular kinetic model.[36] The hydrodynamic model excludes a small zone of a characteristic size l as the no-slip condition is violated in the neighborhood of the contact line.[37−39] Cox has provided the most elaborated description,[38] but a simplified version, due to Voinov, works well for dynamic contact angles not exceeding 130°. Voinov's equation reads[37]

$$\theta^3 = \theta_0^3 + 9\frac{\mu u}{\gamma}\ln\frac{L}{l} \tag{3}$$

Where μ is the viscosity of the moving liquid and L is a macroscopic length scale. The molecular-kinetic theory considers the molecular jumps at the contact line as a rate-activated process and derives the following relation:[40−42]

(10) Kedzierski, J.; Berry, S. *Langmuir* **2006**, *22*, 5690.
(11) Berry, S.; Kedzierski, J.; Abedian, B. *J. Colloid Interface Sci.* **2006**, *303*, 517.
(12) Jackel, J. L.; Hackwood, S.; Veselka, J. J.; Beni, G. *Appl. Opt.* **1983**, *22*, 1765.
(13) Berge, B.; Peseux, J. *Eur. Phys. J. E* **2000**, *3*, 159.
(14) Satoh, W.; Yokomaku, H.; Hosono, H.; Ohnishi, N.; Suzuki, H. *J. Appl. Phys.* **2008**, *103*, 034903/1.
(15) Khare, K.; Herminghaus, S.; Baret, J.-C.; Law, B. M.; Brinkmann, M.; Seemann, R. *Langmuir* **2007**, *23*, 12997.
(16) Hayes, R. A.; Feenstra, B. J. *Nature* **2003**, *425*, 383.
(17) Hayes, R. A.; Feenstra, B. J.; Camps, I. G. J.; Hage, L. M.; Roques-Carmes, T.; Schlangen, L. J. M.; Franklin, A. R.; Valdes, A. F. *Dig. Tech. Pap. - Soc. Inf. Disp. Int. Symp.* **2004**, *35*, 1412.
(18) Sun, B.; Heikenfeld, J. *J. Micromech. Microeng.* **2008**, *18*, 025027/1.
(19) Nisar, A.; Afzulpurkar, N.; Mahaisavariya, B.; Tuantranont, A. *Sens. Actuators, B* **2008**, *B130*, 917.
(20) Chen, L.; Lee, S.; Choo, J.; Lee, E. K. *J. Micromech. Microeng.* **2008**, *18*, 013001/1.
(21) Fair, R. B. *Microfluid. Nanofluid.* **2007**, *3*, 245.
(22) Janocha, B.; Bauser, H.; Oehr, C.; Brunner, H.; Goepel, W. *Langmuir* **2000**, *16*, 3349.
(23) Quilliet, C.; Berge, B. *Europhys. Lett.* **2002**, *60*, 99.
(24) Kuo, J. S.; Spicar-Mihalic, P.; Rodriguez, I.; Chiu, D. T. *Langmuir* **2003**, *19*, 250.
(25) Srinivasan, V.; Pamula, V. K.; Fair, R. B. *Lab Chip* **2004**, *4*, 310.
(26) Berry, S.; Kedzierski, J.; Abedian, B. *Langmuir* **2007**, *23*, 12429.
(27) Antelmi, D. A.; Connor, J. N.; Horn, R. G. *J. Phys. Chem. B* **2004**, *108*, 1030.
(28) Staicu, A.; Mugele, F. *Phys. Rev. Lett.* **2006**, *97*, 167801/1.
(29) Seddon, K. R.; Rogers, R. D. *Ionic liquids: Industrial Applications for Green Chemistry*; American Chemical Society: Washington, D.C., 2002.
(30) Seddon, K. R.; Rogers, R. D. *Ionic liquids III: Fundamentals, Progress, Challenges, and Opportunities*; American Chemical Society: Washington, D.C., 2005.
(31) Rogers, R. D.; Seddon, K., R. *Science* **2003**, *302*, 792.
(32) Rogers, R. D.; Seddon, K. R. *Ionic Liquids as Green Solvents*; American Chemical Society: Washington, D.C., 2003.
(33) Ohno, H. *Electrochemical Aspects of Ionic Liquids*; Wiley-Interscience: Hoboken, N.J., 2005.
(34) Millefiorini, S.; Tkaczyk, A. H.; Sedev, R.; Efthimiadis, J.; Ralston, J. *J. Am. Chem. Soc.* **2006**, *128*, 3098.
(35) Paneru, M.; Priest, C.; Sedev, R.; Ralston, J. *J. Phys. Chem. C* **2010**, *114*, 8383.
(36) Ralston, J.; Popescu, M.; Sedev, R. *Ann. Rev. Mater. Res.* **2008**, *38*, 23.
(37) Voinov, O. V. *Fluid Dyn.* **1976**, *11*, 714.
(38) Cox, R. G. *J. Fluid Mech.* **1986**, *168*, 169.
(39) de Gennes, P. G. *Colloid Polym. Sci.* **1986**, *264*, 463.
(40) Blake, T. D.; Haynes, J. M. *J. Colloid Interface Sci.* **1969**, *30*, 421.

$$\cos\theta = \cos\theta_0 - \frac{2k_BT}{\gamma\lambda^2}\sinh^{-1}\frac{u}{2k_0\lambda} \quad (4)$$

where λ is the average size of the molecular jump, k_0 the jump frequency at $u = 0$, k_B is Boltzmann constant, and T is absolute temperature. In general, both viscous and molecular dissipation should be taken into account,[42,43] but in practice, the above two approaches are considered as alternatives.

In this work, we have used an ionic liquid (1-butyl-3-methylimidazolium tetrafluoroborate) immersed in hexadecane and performed electrowetting on Teflon AF1600 surfaces. The system showed extremely robust electrowetting behavior: large contact angle variations (up to 130°), excellent reversibility, and negligible contact angle hysteresis. DC and AC voltages produced similar results but lower contact angles could be reached with AC voltage. Spreading and retracting of the ionic liquid droplet was very quick and we speculate about the dissipation mechanisms operating under electrowetting conditions.

Materials and Methods

Glass slides (unpolished float glass slides) coated with 30 nm indium tin oxide (ITO), obtained from Delta Technologies (Stillwater, MN), were cleaned with isopropanol, dried in a stream of filtered nitrogen, and dip-coated with Teflon AF1600 (DuPont Fluoroproducts, Wilmington, DE). The coating solution consisted of 6% AF1600 dissolved in perfluoro-2-butyl tetrahydrofuran (Fluorinert FC-75, Derbyshire, U.K.). The slides were immersed in the coating solution at a speed of 200 μm/s and, after a 15 s pause, withdrawn at the same speed. After withdrawal, the slides were dried for 30 min in a laminar flow cabinet and then dried at 100 °C for 30 h. The thickness of the AF1600 layer was determined by capacitance measurements. The capacitance, C, of a 10 μL droplet of 0.1 M KCl was measured with a HP Impedance Analyzer (HP4192A) while the base diameter of the droplet, $2b$, was determined from an optical image. The film thickness was calculated as $\varepsilon\varepsilon_0\pi b^2/C$, where ε_0 is the permittivity of vacuum, and ε (= 1.93[44]) is the dielectric constant of AF1600. The value of the thickness was confirmed using a stylus profilometer (Zeiss HandySurf) to obtain the profile of a step made in the AF1600 film. The average film thickness was 3.8 ± 0.2 μm.

Prior to use, the hexadecane (99%, Sigma-Aldrich) was filtered through a column containing aluminum oxide powder (BDH). The ionic liquid used was 1-butyl-3-methylimidazolium tetrafluoroborate (bmim.BF_4; molecular mass 226.02 g/mol, density 1.21 g/cm^3, viscosity 180 mPa·s[45]). The ionic liquid was purified by extraction with charcoal powder, filtering through a 0.2 μm Teflon filter, extraction with ethyl acetate, and evacuated under medium vacuum (0.1 mbar) for about 24 h.[46]

The coated slide (insulated electrode) was loaded into a home-built cell (Figure 1) filled with hexadecane. The cell was then placed in a customized sessile drop apparatus and a 10 μL droplet of bmim.BF_4 was formed using a micropipet (Eppendorf). A platinum needle was inserted in the droplet and a potential difference between the droplet and the insulated ITO electrode was applied. Potentials were typically increased and decreased in increments of 10 V using a power supply and an amplifier (Trek 610D, Medina, NY). A signal generator (Kenwood, CR Oscillator, AG-203) was used to generate AC potentials (frequency 500 Hz, sine or square waves). The voltage output was connected to the ITO electrode while the platinum needle, that is, the droplet, was grounded. For each electrowettting curve (contact angle versus voltage), the voltage was increased from zero to the maximum achievable value (positive, negative or rms) until contact angle saturation was reached. A fresh solid surface was used for every measurement unless stated otherwise.

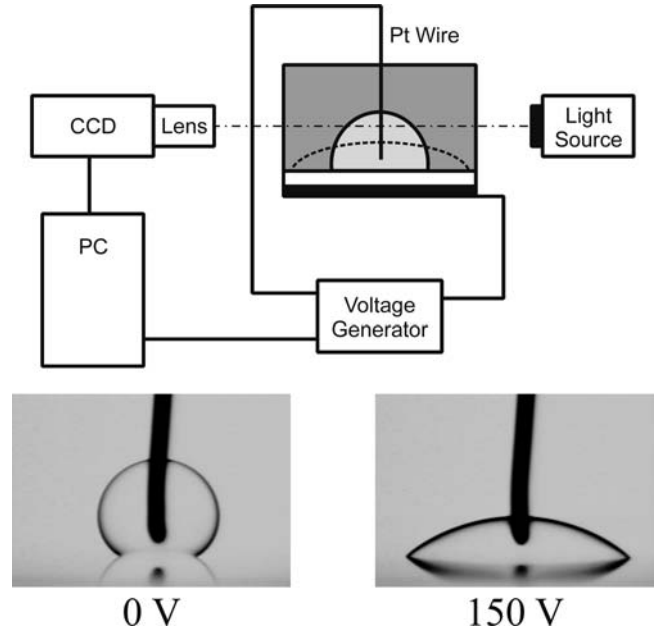

Figure 1. Schematic diagram of the experimental setup. The photographs show a droplet of ionic liquid (bmim.BF_4) immersed in hexadecane on Teflon AF1600 at 0 and 150 V DC.

The sessile drop method[47] and the capacitance technique[4,44] were combined for the measurement of static contact angles. The profile of the droplet resting on the surface was captured with a digital camera (JAI, CV-M10BX). Contact angles were determined by drawing a tangent to the profile at the contact line using ImageJ (a public domain image processing program[48]). These values were plotted against capacitance values measured using an impedance analyzer (Hewlett-Packard model 4192A) to obtain a calibration curve for a given droplet volume. These calibrated values were then used to obtain the contact angles from capacitance measurements. Dynamic spreading (wetting) and retraction (dewetting) were filmed with a high-speed camera (Olympus Encore MAC-2000) at 1000 frames/s.

All experiments were carried out at room temperature (24 °C) in a class 1000 clean room (humidity ~45%).

Results

The electrowetting curve for bmim.BF_4 on Teflon AF1600 in hexadecane is shown in Figure 2. The contact angle at zero external voltage (measured through the ionic liquid) is 145° ± 5°, indicating that the surface is preferentially wetted by the alkane. A DC voltage was applied in increments of 10 V from zero to 250 V and back. The positive and negative branches of the electrowetting curve were recorded on the same location on the sample. The contact angles obtained with the increasing voltage are static advancing measurements and those obtained with a decreasing voltage are static receding ones. The difference between advancing and receding contact angle is called contact

(41) Blake, T. D. *Surfactant Sci. Ser.* **1993**, *49*, 251.
(42) Blake, T. D. *J. Colloid Interface Sci.* **2006**, *299*, 1.
(43) Brochard-Wyart, F.; de Gennes, P. G. *Adv. Colloid Interface Sci.* **1992**, *39*, 1.
(44) Quinn, A.; Sedev, R.; Ralston, J. *J. Phys. Chem. B* **2003**, *107*, 1163.
(45) Endres, F.; Abbott, A. P.; MacFarlane, D. R. *Electrodeposition from Ionic Liquids*; Wiley-VCH: Weinheim, 2008.
(46) Lockett, V.; Sedev, R.; Ralston, J.; Horne, M.; Rodopoulos, T. *J. Phys. Chem. C* **2008**, *112*, 7486.
(47) Adamson, A. W.; Gast, A. P. *Physical Chemistry of Surfaces*, 6th ed.; Wiley: New York, 1997.
(48) Rasband, W. S. ImageJ, U.S. National Institutes of Health: Bethesda, MD; http://rsbweb.nih.gov/ij/index.html, 2009.

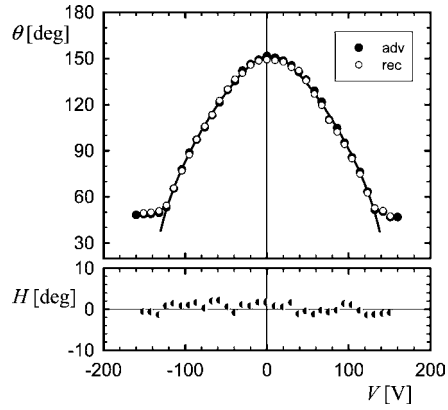

Figure 2. Static contact angle, θ, as a function of the applied DC voltage, V, for a droplet of ionic liquid immersed in hexadecane on Teflon AF1600. Voltage was gradually increased and then decreased back to zero (in steps of 10 V) in order to obtain the advancing and receding contact angles. The solid line is the best fit of the Young-Lippmann eq 1. The lower graph shows contact angle hysteresis, $H = \theta_A - \theta_R$, vs applied voltage, V.

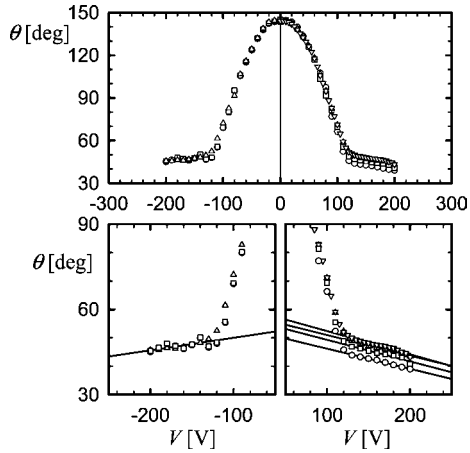

Figure 3. Electrowetting curves (contact angle vs voltage) obtained with DC voltage (Teflon AF1600/bmim.BF_4/Hexadecane). The lower graphs are expanded portions of the upper curve, showing repeated electrowetting at one and the same location on the insulated electrode.

angle hysteresis and is a sensitive measure of the nonideality of the system. The AF1600/bmim.BF_4/alkane system displays a very low hysteresis: 2° (Figure 2, bottom). The electrowetting curve follows the Young-Lippmann equation (solid line in Figure 2, top) up to voltages of magnitude 130 V. Beyond this threshold, the contact angle is almost independent of the applied voltage. This effect is known as contact angle saturation and occurs at $V_S = \pm 130$ V and $\theta_S = 48°$.

Electrowetting experiments with DC voltage were repeated at the same location for both positive and negative potentials and the results are shown in Figure 3. For negative potentials, the saturation angle was not affected. For positive potentials, the saturation contact angle slightly increased during subsequent experiments. Electrowetting curves were recorded with various voltage increments, from 5 to 100 V, in both positive and negative direction without detecting any significant difference.

Electrowetting experiments were also carried out using AC potentials. The AC frequency was varied between 100 and 1000 Hz using both sinusoidal and square waveforms. No significant influence of the signal type or frequency was observed. The contact angle as a function of the rms voltage of a 500 Hz square wave is shown in Figure 4. The AC voltage was cycled from

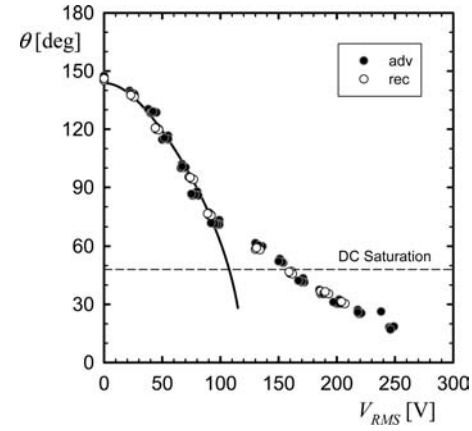

Figure 4. Electrowetting curve (contact angle vs rms voltage) for Teflon AF1600/ /bmim.BF_4/Hexadecane obtained with AC voltage (square wave, 500 Hz). Five consecutive experiments, carried out on the same location on the Teflon-coated electrode, are shown to illustrate the robustness of the operation. The solid line is the best fit of the Young-Lippmann eq 1. The dotted line indicates the saturation contact angle obtained with DC voltage.

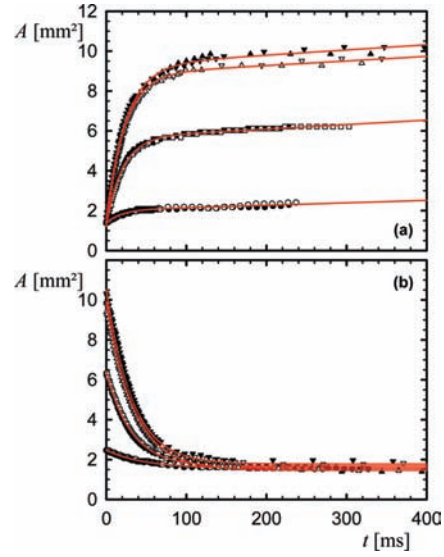

Figure 5. Base area, A, vs time, t, for a droplet of ionic liquid immersed in hexadecane on a flat Teflon-coated electrode, subjected to a DC voltage step (○, 50 V; ●, −50 V; □, 100 V; ■, −100 V; △, 150 V; ▲, −150 V; ▽, 200 V; ▼, −200 V): (a) spreading droplet; (b) retracting droplet. The solid lines are the best fits of (a) $A = a + b[1 - \exp(-t/\tau)] + kt$ (exponential saturation with four free parameters); (b) $A = a + b\exp(-t/\tau)$ (exponential decay with three free parameters).

zero to 250 V and back to zero. Five sets of experimental results were obtained at one and the same location on the solid electrode and the reproducibility was excellent (Figure 4). The AC experiments gave results similar to those obtained in the DC experiments at lower voltages (up to 100 V). At higher voltages, a larger reduction in contact angle was seen for AC potentials. In AC experiments, the saturation contact angle is less than 15° (with DC potentials $\theta_S = 48°$). AC electrowetting exhibited almost no hysteresis, and as in DC, complete reversibility was observed even after reaching the saturation voltage.

The dynamics of spreading and retraction of the ionic liquid droplet is illustrated in Figure 5 with the base area of the droplet, A. The base area (area of the Teflon/IL interface) increases sharply and then more gradually, leading to the final area at which the final contact angle (corresponding to the electrowet-

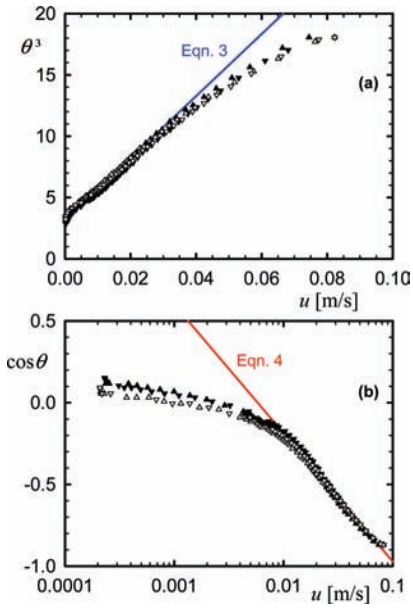

Figure 6. Dynamic contact angle, θ, vs contact line speed, u (△, 150 V; ▲, −150 V; ▽, 200 V; ▼, −200 V): (a) hydrodynamic approach, the line illustrates Voinov's eq 3; (b) molecular-kinetic approach, the line shows the exponential approximation of Blake's eq 4.

ting curve in Figure 2) is established. When the voltage is switched off, the droplet relaxes to its original position. Once the voltage exceeds V_S, all curves merge. Polarity has no influence on the curve (open and filled symbols) below V_S but a subtle difference is seen at $V > V_S$. For retraction, polarity is irrelevant (the voltage is switched off), and in all cases, the droplet retracts to the same initial value of the contact angle.

The dependence of the dynamic contact angle, θ, on the speed of the contact line, u, can be extracted from the results shown in Figure 5. The contact line speed was obtained from the derivative of the base area: $u = db/dt = [2(\pi A)^{1/2}]^{-1}\, dA/dt$. The instantaneous contact angle was calculated from the base area and the fixed droplet volume assuming the droplet shape at any time was that of a spherical cap. The results obtained for a droplet spreading at 150 and 200 V are presented in Figure 6. The format of the graphs should linearize eqs 3 and 4. The results obtained at speeds of up to 0.04 m/s are well accounted for by the hydrodynamic description. The kinetic dependence in the range of higher speeds (>0.01 m/s) is better represented by the molecular-kinetic equation.

Discussion

A key difference between SLV and SLL systems is that the electrowetting term in eq 1, at fixed voltage and insulator thickness, is more significant simply because the liquid/liquid interfacial tension ($\gamma_{IL/HD} = 21.7$ mJ/m^2) is lower than the liquid/air surface tension ($\gamma_{IL/air} = 67.0$ mJ/m^2). Thus, by simply replacing air with hexadecane, the electrowetting effect is enhanced by a factor $\Delta \cos \theta_{SLL}/\Delta \cos \theta_{SLV} = \gamma_{IL/air}/\gamma_{IL/HD} \approx 3$.

An important outcome of this work is the very large contact angle changes observed: from about 150° down to 48° (when using DC voltage, Figure 2) and further down to less than 15° (when using AC voltage, Figure 4). These changes are much larger than what we have observed in amorphous Teflon/conductive liquid/air systems (from 115° to 70° for three grades of amorphous Teflon/0.1 M KCl/air[2,44] and from 70° down to 50° for AF1600/ionic liquid/air[34]). One key difference between SLV and SLL systems is the larger initial contact angle, θ_0. Hexadecane wets preferentially the hydrophobic surface (AF 1600) and the contact angle at zero external voltage, θ_0, is large. Since both hexadecane and Teflon are apolar materials,[49] that is, they interact through dispersive forces only, Fowkes approach[47] can be used to relate the interfacial tension, γ_{12}, to the surface tension of the two separate materials, γ_1 and γ_2:

$$\gamma_{12} = \gamma_1 + \gamma_2 - 2(\gamma_1\gamma_2)^{1/2} \qquad (5)$$

Using the surface tensions of hexadecane (27.6 mJ/m^2) and Teflon AF1600 (12.4 mJ/m^2[22]), we estimate the interfacial tension of the AF1600/HD interface at 3.0 mJ/m^2. By inserting $\theta_0 = 150°$ and $\gamma_{IL/HD} = 21.7$ mJ/m^2 into Young's equation, we obtain the AF1600/bmimBF$_4$ interfacial tension to be $\gamma_{S/IL} = 21.8$ mJ/m^2. In other words, the force driving the spreading of the ionic liquid on the Teflon surface, prewet with the alkane, is very small in the absence of external voltage. Because $\gamma_{IL/HD} \approx \gamma_{S/IL}$, it is plausible that the droplet of ionic liquid rests on a thin film of hexadecane. Quilliet and Berge[23] estimated theoretically that this is possible by considering van der Waals and electrostatic interactions. The refractive indices of bmim.BF$_4$ (1.421) and hexadecane (1.434) are very similar and the Hamaker constants for the two materials should not be significantly different.[50]

Another key feature of our results is the very low contact angle hysteresis, within 2° for both DC (Figure 2) and AC voltages (Figure 4). This is appreciably less than what we have seen in low-hysteresis ($\theta_A - \theta_R < 10°$) Teflon/aqueous salt/vapor systems.[2,44] There was no significant change with voltage or a difference between the DC and AC voltage experiments as seen in SLV electrowetting.[51] Contact angle hysteresis is a macroscopic manifestation of the imperfections of the solid surface and can be very large.[47] Verheijen and Prins[4] reported a very low hysteresis (within 2°) on a AF1600 surface electrowetted with an aqueous salt solution in air, but their solid surface was impregnated with silicone oil prior to the SLV electrowetting experiment. Unusually, low hysteresis during electrowetting in SLL systems was found by Berge and Peseux[13] and they attributed the fact to a residual thin liquid film trapped under the electrowetted droplet. Maillard et al.[52] observed a hysteresis of 2° or less in various SLL systems as long as the contact angle at zero voltage was larger than 160°. Microfluidic experiments[21,25] have shown that electrowetting in ambient oil (instead of air) significantly reduces evaporation, contamination, biofouling, and improves droplet transport. Static and transient capacitance measurements demonstrated convincingly the presence of an oil film.[21] It is apparent that electrowetting in SLL systems has enormous practical advantages. Janocha et al.[22] reported very large contact angle changes in SLL electrowetting. The water contact angle against decane dropped from 160−170° to about 80° on both polyethylene and polypropylene surfaces. In both cases, the hysteresis was small (~2°) and the electrowetting curve prior to saturation was well-described by Young-Lippmann equation.

Our results show very low hysteresis (Figures 2 and 4) but also a total reversibility with respect to the voltage applied. It

(49) van Oss, C. J. *Interfacial Forces in Aqueous Media*, 2nd ed.; Taylor & Francis: Boca Raton, FL, 2006.
(50) Israelachvili, J. N. *Intermolecular and Surface Forces*, 2nd ed.; Academic Press: London, 1991.
(51) Li, F.; Mugele, F. *Appl. Phys. Lett.* **2008**, *92*, 244108/1.
(52) Maillard, M.; Legrand, J.; Berge, B. *Langmuir* **2009**, *25*, 6162.

should be noted that reversibility is found even after exceeding the saturation voltage. This implies that charge injection, which is often invoked as the major cause for saturation,[4] was not significant in our experiments. Again, the possible presence of a thin alkane film intervening between the ionic liquid and the insulating polymer may be a key factor.

Our results are well-described by the Young-Lippmann eq 1. The solid lines shown in Figures 2 and 4 are the least-squares fits obtained by using the equation $\cos\theta = \cos\theta_0 + \alpha(\varepsilon\varepsilon_0/\gamma d)V^2$ and treating θ_0 and α as adjustable parameters. Since all quantities belonging to the electrowetting term are known, we estimated $\alpha = 0.45$. As argued previously,[2,44] the closeness of α to 1/2 is an indication of the quality of the experimental data. Thus, Young-Lippmann equation provides a consistent description of the electrowetting curve provided that the saturation voltage is not exceeded.

We have argued[2] that the saturation limit in SLV systems can be estimated from eq 2. For the system considered here, the zero-interfacial-tension hypothesis is written as

$$\theta_S = \arccos\frac{\gamma_{S/HD}}{\gamma_{IL/HD}} \approx 82^\circ \qquad (6)$$

This value may be a crude estimate of the inflection point of the AC electrowetting curve[35] (Figure 4), but it is certainly different from the saturation contact angle we measured under DC ($\theta_S = 48^\circ$) and AC ($\theta_S \leq 15^\circ$) voltages.

Following the original suggestion by Berge and Peseux,[13] we suppose the nominal Teflon/ionic liquid interface contains alkane patches, that is, the droplet/electrode contact has been breached by residual patches of hexadecane. The interfacial tension of such a composite surface would include Teflon/IL and IL/HD contributions, but these are energetically equivalent (see above) and will not affect appreciably the above prediction. As a matter of fact, even a precise value of $\gamma_{S/IL}$ would not improve the predicted saturated contact angle, as this interfacial tension does not appear in eq 6. The predicted value θ_S would be closer to the experimental value only if the interfacial tension $\gamma_{S/HD}$ was larger. Thus macroscopic energetic considerations suggest the ionic liquid is spreading ahead of the macroscopic droplet. We have no experimental evidence for the formation of such a precursor. Moreover, such a picture contradicts the ample evidence that an oil film is present beneath the electrowetting droplet.[13,21,28] It would be useful to reconsider the zero-interfacial-tension hypothesis in conjunction with a Frumkin-Derjaguin model of the contact line[53,54] (i.e., including the role of thin wetting films).

When AC voltage is used, saturation is postponed and truly low contact angles can be reached (Figure 4). We have shown that SLL electrowetting of bmim.BF_4−water mixtures on Teflon AF1600 yields a constant saturation contact angle under DC voltage and different angles under AC voltage.[35] It seems that further experimentation, particularly with diverse ionic liquids, might be useful in clarifying the issue of saturation in electrowetting. Hong et al.[55] provided an explanation for the superior performance of AC voltage in electrowetting. They modeled numerically the AC field inside a droplet electrowetted on an insulator. When an AC voltage was used to achieve a contact angle change identical to that obtained with DC voltage, the local electric field near the contact line is weaker and does not trigger contact angle saturation. Our experiments were conducted at frequencies lower than those considered by Hong et al. (1−16 kHz[55]) and also in ambient hexadecane rather than air. Nevertheless, their model provides a qualitative rationalization for the different role of AC and DC voltages seen in our experiments (Figures 2 and 4).

A further confirmation of the superior performance of the SLL system studied here, particularly with respect to reversibility, is shown in Figure 3. Repeated runs on one and the same location of the sample yielded exactly the same result. Variations in the voltage increment used (from 5 to 50 V) in the electrowetting experiment had no effect on the electrowetting curve. This is in marked contrast with the influence detected in SLV systems.[2] The system studied here is also quite resilient beyond the saturation threshold where the electrowetting curve deviates from the Young-Lippmann equation (Figure 3). A subtle influence of the voltage sign is found. For negative polarizations, beyond V_S, the contact angle diminishes linearly with voltage and the curve can be retraced time after time. For positive voltages, a linear decrease is also seen, but the response shifts ever so slightly upward (about 5° in total). This is reminiscent of the asymmetry seen in SLV systems containing ionic liquids.[34] We have previously reported differences between negative and positive polarization in AF1600/aqueous KCL/air systems and attributed the effect to specific adsorption of hydroxyl ions.[44] Following this line of reasoning, we conclude that the tetrafluoroborate anion interacts with the Teflon surface specifically, but it is detectable only above saturation voltage.

The electrowetting curves obtained with AC voltage show very little hysteresis (≤1°), excellent reversibility, and reduced saturation angles (Figure 4). To avoid the influence of stray capacitance (which can limit the actual voltage across the insulator and thus weaken the electrowetting effect at high frequency) and the unnecessary fluctuations of the droplet (at low frequency the liquid shape follows the voltage oscillations), we limited the AC frequency within the window 100−1000 Hz. Within this range, the electrowetting curve is independent of the frequency and the form of wave used (sinusoidal, square or triangular). At lower voltages ($V \leq 100$ V), the difference between AC and DC curves is nonexistent (Figure 4). However, at higher voltages, they diverge. The minimum AC contact angle is much smaller and close to zero. To the best of our knowledge, this is the lowest contact angle achieved with electrowetting[35] (earlier reports indicated a limit of about 30° for salty water on PET[56] and PTFE[5,56] in air). From a practical point of view, this system, with its robust behavior under AC voltage, is an excellent candidate for implementation in devices (e.g., valves or actuators) where a maximum change in capillary force is required.

One of the most attractive features of electrowetting is that it is fast. The dynamics of spreading at constant applied DC voltage is illustrated in Figure 5. We assume that at any applied V the surface charge density reaches a maximum value σ_{max}, determined by the maximum ion concentration at the Teflon/ionic liquid interface. The base area, A (which reflects the instantaneous dynamic contact angle), then increases until the contact angle attains the static value at that voltage. The kinetic curves (contact angle versus time) for both spreading (Figure

(53) Churaev, N. V.; Sobolev, V. D. *Adv. Colloid Interface Sci.* **1995**, *61*, 1.
(54) Starov, V. M.; Velarde, M. G.; Radke, C. J. *Wetting and Spreading Dynamics*; CRC: Boca Raton, FL, 2007.
(55) Hong, J. S.; Ko, S. H.; Kang, K. H.; Kang, I. S. *Microfluid. Nanofluid.* **2008**, *5*, 263.
(56) Vallet, M.; Berge, B.; Vovelle, L. *Polymer* **1996**, *37*, 2465.

5a) and retraction (Figure 5b) follow an essentially exponential behavior. In the advancing case (spreading), a linear trend was added to account for the much slower second stage of the spreading ($t > 120$ s). The final area (A at $t \rightarrow \infty$) is proportional to the applied voltage, V. An exponential growth of the base area of the droplet has been found in various spontaneous spreading experiments, for example, liquid droplets in air on various surfaces,[57] air bubbles,[58,59] or oil droplets[60] on a solid surface under water. Apparently, the external voltage improves the wettability of the system but does not affect the mode of spreading (wetting) or retracting (dewetting). In other words, under a fixed DC voltage, the electrowetting droplet spreads in much the same way as does a nonelectrified droplet on a wettable substrate.

The limiting value of σ_{max} is of the order of 0.5 mC/m^2. This value is comparable with the one we estimated for Teflon AF1600/aqueous 0.1 M KCl/air systems (0.25 mC/m^2).[44] It is about 1 order of magnitude lower than the value calculated for Teflon AF1600 in 1 mM KCl (5 mC/m^2),[61] the values typically seen in electrokinetic measurements on polymers surfaces (4.8 mC/m^2)[62] or charge injection on polymer surfaces (1.7 mC/m^2),[63] but still an order of magnitude higher than the limiting surface charge possible in air (0.03 mC/m^2).[64]

The characteristic time, τ (in Figure 5) is about 20 ms for spreading and 35 ms for retraction. Experiments with a glycerol−water mixture of a similar viscosity (160 mPa·s) yielded $\tau \approx 20$ ms, thus, suggesting that viscosity is the key parameter determining the rate of spreading rather than any peculiar behavior of the large imidazolium cations. On the other hand, for AF1600/IL/HD, dewetting is visibly slower than wetting (this was not observed in the glycerol−water mixture experiments) which implies that slow relaxation of large cations at the interface has a certain influence. This is further supported by the asymmetry seen in Figure 5a, the area changes slightly faster for positive DC voltages, that is, when the smaller tetrafluoroborate anions are attracted to the polymer surface.

Finally, from the kinetic data $A(t)$, we derive the dependence of the dynamic contact angle, θ, on the contact line speed, u (Figure 6). The initial rate of spreading is as high as 0.08 m/s (and about 3 times lower for retraction). As can be seen in Figure 6a, the hydrodynamic model of Voinov (eq 3) provides a reasonable description up to about $u = 0.04$ m/s. The slope of the line in Figure 6a is about 4 times less than the one estimated through eq 3, but this level of discrepancy is rather common.[36] From a hydrodynamic point of view, the viscosity of both advancing and receding liquids should be taken into account.[38] However, the ionic liquid is so viscous that the viscosity ratio, m, in our experiment ($\mu_{HD}/\mu_{IL} = 0.02$) is effectively the same as for a water droplet spreading in air ($\mu_{air}/\mu_{water} = 0.022$). On the other hand, the exponential version of Blake's molecular-kinetic model (eq 4) performs well at higher velocities of the contact line ($u \geq 0.01$ m/s), Figure 6b. Again, the molecular parameters derived from the best fit shown in Figure 6b (molecular jumps of size $\lambda = 1.1$ nm and frequency, at $u = 0$, $k_0 = 70$ MHz) are reasonable and in line with previous reports.[36,42]

Staicu and Mugele[28] provided a detailed study of a silicone oil film entrapped between the aqueous droplet (aqueous NaCl) and the insulating polymer layer (Teflon AF1600). The oil film is initially thick (of the order of 400 nm), quickly becomes unstable, and breaks into small droplets. We note that in these experiments the voltage was ramped up before the droplet had contacted the insulated electrode. This protocol is likely to create a thinning oil film, especially in view of the very high viscosity ratio ($m \approx 100$). Thick oil films ($\sim$10 μm) and their instability under electrowetting conditions have been used to improve the performance of electrowetting display pixels.[18]

We position our droplet on the surface of the electrode and wait for a steady state to be established, which we characterize with the static contact angle at zero external voltage, θ_0. Only then, we apply a fixed voltage step and consider the dynamics of the contact line. We cannot rule out the existence of a very thin hexadecane film during our forced spreading experiments (this should be tested in a separate experiment). However, its thickness must be very small because θ_0 is large but significantly lower than 180° (Figures 2 and 4); the electrostatic pressure is always destabilizing,[23,65] especially at high ionic strength in the droplet (ionic liquids create high ionic strength).[33] If an oil film of nanometre thickness exists, the disjoining pressure inside this wetting film must be significant and the system is still a three-phase one: solid/liquid/film (see Starov et al.[54] for details). The presence of such a thin wetting film would not invalidate the macroscopic phenomenology of spreading discussed here.

Finally, the kinetics of wetting observed during spreading (under a constant DC voltage exceeding the saturation value) fits well with the qualitative concept formulated by Brochard-Wyart and de Gennes,[43] which includes both viscous, D_1, and molecular dissipation, D_2 (p is a numerical constant):

$$\frac{D_1 + D_2}{\mu u^2} = \frac{p}{\theta} \ln \frac{L}{l} + \exp\left(\frac{\lambda^2 W_A}{k_B T}\right) \qquad (7)$$

The first term depends on the dynamic contact angle, θ, and as the liquid edge becomes thinner during spreading, the angle decreases and the importance of the viscous term increases sharply.[39] At the same time, molecular dissipation (2nd term) is not strongly affected by the contact angle[42,66] and the total balance is shifted toward a dominant viscous dissipation whenever θ is small. In our case, viscous dissipation is more significant at low speeds (later stages of the spreading) when the contact angle is relatively small. During the initial stages of the electrowetting, the contact line speed is high but the dynamic contact angle is quite large and molecular dissipation prevails. A good contrasting example is provided by the recent work of Fetzer and Ralston[59] on the receding contact line formed when an emerging bubble encounters a hydrophobic solid surface. In their case, hydrodynamic dissipation was prominent at high speed while molecular dissipation dominated when contact line movement slowed down. From the reasoning given above, it appears that viscous dissipation dominated their results because the initially high speed coincided with small contact

(57) Dodge, F. T. *J. Colloid Interface Sci.* **1988**, *121*, 154.
(58) Phan, C. M.; Nguyen, A. V.; Evans, G. M. *Langmuir* **2003**, *19*, 6796.
(59) Fetzer, R.; Ralston, J. *J. Phys. Chem. C* **2009**, *113*, 8888.
(60) Fetzer, R.; Ramiasa, M.; Ralston, J. *Langmuir* **2009**, *25*, 8069.
(61) Zimmermann, R.; Dukhin, S.; Werner, C. *J. Phys. Chem. B* **2001**, *105*, 8544.
(62) Van Wagenen, R. A.; Coleman, D. L.; King, R. N.; Triolo, P.; Brostrom, L.; Smith, L. M.; Gregonis, D. E.; Andrade, J. D. *J. Colloid Interface Sci.* **1981**, *84*, 155.
(63) Fowkes, F. M.; Hielscher, F. H. *Org. Coat. Plast. Chem.* **1980**, *42*, 169.
(64) Cross, J. A. *Electrostatics: Principles, Problems and Applications*; Adam Hilger: Bristol, 1987.
(65) Herminghaus, S. *Phys. Rev. Lett.* **1999**, *83*, 2359.
(66) Blake, T. D.; De Coninck, J. *Adv. Colloid Interface Sci.* **2002**, *96*, 21.

angles (as measured through the water), in accordance with eq 7. As contact line speed decreased during the dewetting of the hydrophobic substrate, the dynamic contact angle gradually increased and molecular dissipation became the leading contribution.

Conclusion

A droplet of ionic liquid (bmim.BF_4) was immersed in an immiscible liquid (*n*-hexadecane) and was electrowetted on a flat Teflon AF1600-coated electrode. The static contact angle decreases significantly when voltage is applied: from 150° down to 48° (DC voltage) and 15° or less (AC voltage). The reversibility of electrowetting was excellent and contact angle hysteresis was very small (∼2°). The step size used in applying a DC voltage and the polarity of the voltage were not significant. AC electrowetting is very effective and robust, and may offer significant advantages if implemented in microfluidic devices. The electrowetting behavior of this system is similar to that observed in other SLV and SLL systems (symmetric electrowetting curve, accordance with Young-Lippmann equation below saturation). The saturation contact angle could not be predicted with the simple version of the zero-interfacial tension theory.

Electrowetting proceeded very quickly (initial contact line speed reached 0.08 m/s). The base area of the droplet (at a fixed DC voltage) varied exponentially during both spreading (exponential saturation) and retraction (exponential decay, after the voltage was switched off). The characteristic time was 20 ms for spreading (wetting) and 35 ms for retraction (dewetting). The dynamic contact angle versus contact line speed dependence during spreading was correctly described by the hydrodynamic model (Voinov's equation) for small contact angles and by the molecular-kinetic model (Blake's equation, exponential approximation) for large contact angles. The role of viscous and molecular dissipation follows the scheme proposed by Brochard-Wyart and de Gennes.

Acknowledgment. Financial support through The Australian Research Council Special Research Centre Scheme is gratefully acknowledged.

JA9106397